

Deep learning for track recognition in pixel and strip-based particle detectors

O. Bakina¹ D. Baranov¹ I. Denisenko¹ P. Goncharov^{2,1} A. Nechaevskiy¹ Yu. Nefedov¹
 A. Nikolskaya³ G. Ososkov¹ D. Rusov² E. Shchavelev³ S. S. Sun^{4,5} L. L. Wang^{4,5} Y. Zhang⁴
 A. Zhemchugov¹

¹*Joint Institute for Nuclear Research, protect
 Russia, 141980, Dubna, Moscow region, 6 Joliot-Curie St.*

²*Dubna State University,
 19 Universitetskaya St., Dubna, Moscow Region, 141982, Russia*

³*St Petersburg State University,
 7-9 Universitetskaya Emb., St Petersburg 199034, Russia*

⁴*Institute of High Energy Physics CAS,
 19B Yuquan Road, Shijingshan District, Beijing, 100049, China*

⁵*University of Chinese Academy of Sciences,
 19A Yuquan Road, Shijingshan District, Beijing, 100049, China*

E-mail: zhemchugov@jinr.ru

ABSTRACT: The reconstruction of charged particle trajectories in tracking detectors is a key problem in the analysis of experimental data for high-energy and nuclear physics. The amount of data in modern experiments is so large that classical tracking methods, such as the Kalman filter, cannot process them fast enough. To solve this problem, we developed two neural network track recognition algorithms based on deep learning architectures for local (track by track) and global (all tracks in an event) tracking in pixel and strip-based particle detectors. These algorithms were tested using the GEM tracker of the BM@N experiment at JINR (Dubna) and the cylindrical GEM inner tracker of the BESIII experiment. The RDGraphNet neural network model for global track finding, based on a reverse directed graph, showed encouraging results: 98% recall and 86% precision for track finding. The TrackNETv2 local neural network model was supplemented by an additional neuro-classifier was introduced to filter out false tracks. Preliminary tests demonstrated a recall value of 99% at the first stage. After applying the neuro-classifier, the precision was 77% with a slight decrease in the recall to 94%. This result can be improved after further model optimization.

KEYWORDS: Track reconstruction, GEM detectors, Deep learning, Convolutional neural networks, Graph neural networks

Contents

1	Introduction	1
2	TrackNETv3 neural network	2
3	RDGraphNet neural network	6
4	Implementation of neural networks and Ariadne library	9
5	Performance study	9
5.1	Tracking detector of the BM@N experiment	9
5.2	Inner tracker of the BESIII experiment	11
6	Conclusion	13
7	Acknowledgement	16

1 Introduction

The reconstruction of charged particle trajectories in tracking detectors is a key problem in experimental data processing for high-energy and nuclear physics. Tracking algorithms have evolved along with the development of experimental facilities and technologies for particle detection. Currently, the most effective tracking methods are based on the Kalman filter [1]. A typical scheme of tracking using the Kalman filter is to find a track seed, then to extrapolate it to the next coordinate detector and find a hit belonging to the track near the extrapolated point. Further, the procedure is repeated taking into account the new found hit. While this method gives an edge of taking into account the inhomogeneity of the magnetic field, multiple scattering and energy losses when a particle passes through the matter, the computational complexity of the Kalman filter and the significant difficulty of its parallel implementation to take advantage of modern hardware inspire the search for alternative methods for finding tracks, especially when the track multiplicity is large.

The first attempt to use artificial neural networks for track reconstruction was made by B. Denby [2], using multilayer perceptrons and Hopfield’s fully connected neural networks. Later, the imperfection of these neural network algorithms, a sharp drop in tracking efficiency with an increase in the noise level, and the multiplicity of events led to the emergence of a modification of Hopfield’s neural network algorithms, called elastic neural networks [3]. Unfortunately, the efficiency of elastic tracking methods strongly depended on the proper choice of an initial approximation. Recently, deep learning methods have become a major focus of attention due to their ability to reveal hidden nonlinear dependencies in data and to the existence of an efficient parallel implementation of linear algebra operations lying in the base of these methods. The application of these methods for track reconstruction looks very promising, although algorithms for “deep

tracking” that surpass classic methods, such as the Kalman filter, in performance have yet to be developed.

The TrackNETv3 and RDGraphNet track recognition algorithms, based on deep learning methods are proposed in this study to find tracks in pixel and strip particle detectors when a track should be recognized from a set of spatial point hits. The performance of these algorithms was studied in application to track finding in the GEM-based tracker of the BM@N experiment [4] at JINR and in the CGEM-based inner tracker of the BESIII experiment [5] at IHEP CAS, Beijing.

2 TrackNETv3 neural network

A typical tracking detector in a fixed target experiment can be represented by a set of coordinate detector planes (Fig. 1). A particle passing through detectors produces hits in space, where the longitudinal coordinate Z of the hit is determined by the detector position, and the transversal position of the hit in the $X - Y$ plane is directly measured in pixel-based detectors or reconstructed from two or more stereo layers of strip-based detectors. Some of the hits can be noise or fake hits, which are inevitable in the case of strip-based readout due to the appearance of illusory strip intersections if the number of tracks is more than one. Having performed a combinatorial spatial

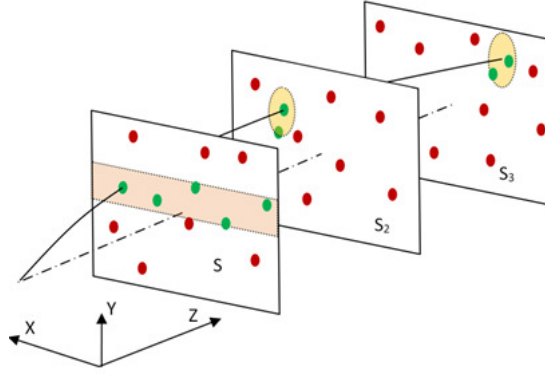


Figure 1: Procedure of track finding in a fixed target experiment using the TrackNET algorithm.

search for track candidates simultaneously using two coordinate projections, one can further use a recurrent neural network (RNN) to separate true and false (ghost) tracks. This two-stage tracking was successfully implemented using Gated Recurrent Units (GRUs) with a somewhat simplified gate mechanism for RNNs [7]. To speed up the search procedure for track candidates, both stages were combined into a single recurrent neural network, TrackNET [8]. Four special neurons were added to the classifier network, performing a prediction of the elliptical region in the next coordinate detector plane, within which it is necessary to search for the continuation of a track candidate. Two of these neurons predict the position of the center of the ellipse, and the other two predict the size of its semi-axes. One more, the fifth output neuron, classifies track candidates into a true track or a ghost one. Combining track extrapolation with testing the hypothesis that the set of hits belongs to the true track and is compatible with a smooth curve essentially reproduces the idea of the Kalman filter with the difference that the physical parameters describing the track are approximated by a neural network using synaptic weights determined during its training.

However, the TrackNET model has some shortcomings. The neural network loss function has three parameters to which it is very sensitive. In addition, the neural network is difficult to train in the case of strip-based readout with many fake hits, since it turns out to be difficult to find a balance between good extrapolation and classification in conditions when the number of false track candidates is substantially larger than the number of real ones. Nevertheless, it is noteworthy that the procedure for predicting an ellipse to find the next hit of a track candidate already gives a hint about the smoothness of the curve. This feature was used to improve the model and resulted in a new TrackNETv2 neural network [9].

The architecture of the TrackNETv2 model is shown in Fig. 2. The input of the neural network is a matrix, where each row contains hit coordinates for a track candidate. The first row of the matrix contains hit parameters in the first detector plane, the second row in the second one, and so on. The size of the matrix is fixed, and the number of rows corresponds to the number of detector planes, except one. The remaining input is padded by zeros.

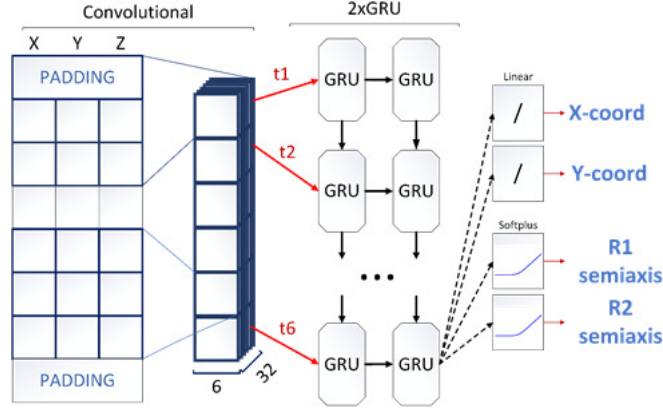


Figure 2: Architecture of the TrackNETv2 model.

The network predicts the position and size of the ellipse, where the next hit of a track candidate is possibly located. The linear activation function is chosen to predict the position of the center of the ellipse, while the softplus [10] activation function is used for semi-axes prediction. The loss function is described by the equation:

$$J = \lambda_1 \cdot \sqrt{\frac{x - x'}{R_1} + \frac{y - y'}{R_2}} + \lambda_2 \cdot R_1 R_2, \quad (2.1)$$

where λ_1, λ_2 are the weights for the equation terms; x', y' are the coordinates of the predicted ellipse center; x, y are the coordinates of the next hit of the current track; R_1, R_2 are the semi-axes of the predicted ellipse.

The loss function allows one to predict the center of the ellipse close to the position of the next hit, simultaneously reducing the size of the semi-axes as much as possible, keeping the true hit within the ellipse.

So far, the layout of a fixed target experiment with coordinate detector planes was considered. When used in a collider experiment with coaxial tracker layers, TrackNETv2 can be adapted in a

trivial way by using cylindrical hit coordinates as an input (X, Y, Z) :

$$Z = R, \quad X = \phi, \quad Y = z, \quad (2.2)$$

where ϕ is in the range of $[-\pi, \pi]$.

The first version of TrackNETv2 was trained with the help of a special bucketing procedure. Tracks were sorted by length. Each group of tracks with a given number of hits in a track was reformed to balance the size of all groups. Randomly selected long tracks were cut and pushed to a bucket with a smaller track length. Thus, buckets with different track lengths (from 3 to the number of stations) were created. Then the last hits of the tracks in every group were selected as labels for the model prediction and loss calculation, while all remaining hits were chosen as inputs. Such a bucketing procedure is unnatural for training recurrent neural networks (RNNs), not even speaking about the need for balancing buckets. According to the structure of RNNs, we decided to recap the training procedure.

At first, the whole true track from Monte-Carlo data, except the last hit, is passed to the input of the model. At the same time, all hits, except the first one, are used as labels for loss function calculation. The model makes predictions for each hit, e.g. for the first hit it will try to predict the ellipse where to search for the second hit, for the first two hits the model tries to guess where the third hit is, etc. Thereby the network predicts ellipses for each timestamp, and we calculate the loss for each model prediction. Then we average the loss value across all timestamps and perform backpropagation. Such a strategy of training is called many-to-many.

There can be samples of different sizes in a single batch of inputs, and we need to pad shorter track candidates to the length of the longest ones across the batch. Usually the padding value equals zero, so if the batch includes two samples with length 4 and length 6, then the candidate with four hits will be extended by the two hits with all three coordinates being zeros. During loss estimation, a special mask for padding is calculated, and these timestamps are excluded from the optimization process.

Switching the training strategy of the TrackNETv2 model forced us to revise the original architecture by removing the convolutional layer. The whole point is that for the receptive size 3 and the "same" padding (1 in this case) at each timestamp, the model is forced to look into the future one step ahead. Thus, if we try to train the network using the many-to-many strategy, the standard convolution will promote the model to cheat during training, and thus the evaluation will fail. We could also make the convolution operation work in a causal way by tuning the padding parameter, however, our study showed that a simple drop of the convolutional layer performed better.

The TrackNETv2 network demonstrates high ($\sim 99\%$) recall, but precision, i.e. the number of ghost tracks, strongly depends on the conditions of the experiment. In the case of few detector layers and a large number of fake hits, the number of ghost tracks becomes unacceptably high. The reason is the high probability to pick up a combination of few fake hits compatible with the track hypothesis. To solve this problem, information about the beam interaction point, giving the primary vertex of the track, would be helpful. However, the model can be trained to use the primary vertex, since this information is also hidden in the data. To do this, TrackNETv2 was supplemented with another classifier, which was trained to give the probability of a track candidate to be a real track. The TrackNETv2 model with the classifier was later called TrackNETv3.

Two independent classifiers were developed (see Fig. 3). For the first classifier (Classifier-GRU), two inputs are used: the output of the second GRU layer of TrackNETv2 and the set of hit coordinates at the end of the track candidate (Last point). Each input is propagated to a fully connected layer (FC). Then the resulting vectors are concatenated (Concat) and transferred to another fully connected layer (FC). All the layers described above use the ReLU activation function [11]. The output of the last FC layer of the classifier uses the softmax [12] activation function.

The input of the second classifier (Classifier-Coords) contains the coordinates of three hits in a track candidate. The first two hits are input for the TrackNETv2, network and the third is the predicted one. These coordinates are concatenated into a vector of size 9 and then fed into a small fully connected block of two layers with ReLU activation. The output of the last FC layer uses the sigmoid [20] activation function.

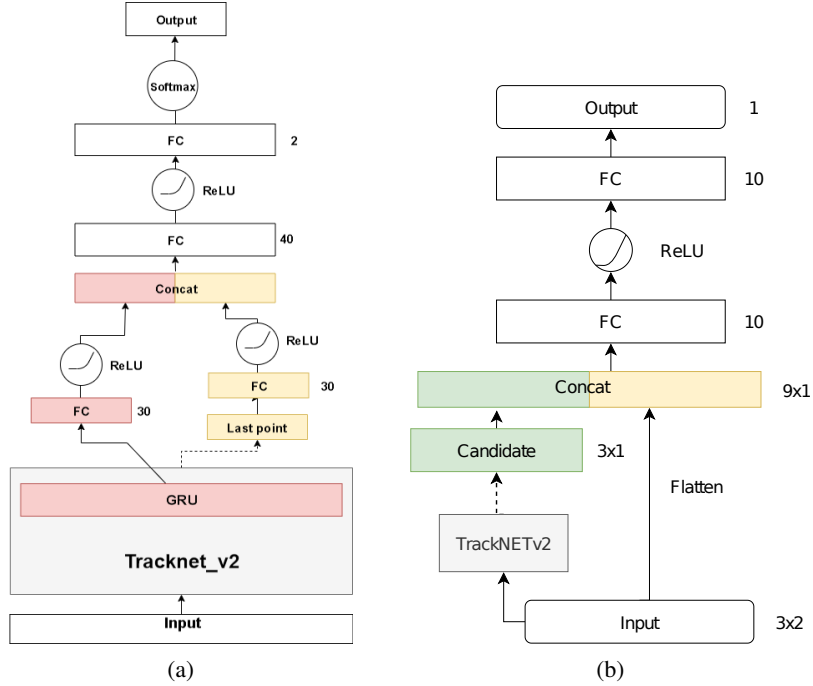


Figure 3: Scheme of the Classifier-GRU (a) and Classifier-Coords (b) classifiers.

To train the classifiers, the proper choice of the loss function is crucial. The binary cross entropy [21] is the standard for binary classification:

$$BCE = - \sum y_t \log(p_t), \quad (2.3)$$

where y_i is the label of the t -th sample, and p_t is the predicted probability. However, the use of this function gives the preference to easy cases with a high probability to be a true track and leads to a weak learning ability. The focal loss function solves this problem by adding the modulating factor γ to the cross entropy value [22]. The idea is that if a sample is already well classified, we can significantly decrease the weight of its contribution to the loss. To set a balance of positive and negative examples, the weighting parameter α is used; it has the meaning of the inverse class

frequency.

$$FL = - \sum y_t (1 - p_t)^\gamma \log(p_t), \quad (2.4)$$

TrackNETv3 with different combinations of classifiers and loss functions was tested and the results are shown in Tab. 1. The results for the TrackNETv2 network tested on the same set are also demonstrated. Clearly, the combination of Classifier-GRU and focal loss function gives the best result. Since any classifier predicts the probability of a track candidate to be a real track, the proper

Table 1: Training results for TrackNETv3.

Classifier	Loss function	Precision	Recall
No classifier	TrackNETLoss	0.01	0.99
Classifier-GRU	Cross Entropy	0.54	0.95
Classifier-GRU	Focal	0.677	0.98
Classifier-Coords	Cross Entropy	0.66	0.94
Classifier-Coords	Focal	0.58	0.96

threshold choice allows adjusting the efficiency and purity of track recognition. For instance, the threshold of 0.55 corresponds to the precision of 0.978 and recall of 0.683.

Another improvement over the original TrackNETv2 model lies in the optimization of the inference. We used the Faiss library [13] for a fast search of hits caught by the predicted ellipse. The model makes ellipse predictions, simultaneously we put all event hits in the search index from Faiss. The next step is to use ellipse centers to find K-nearest hits for each of the centers. After finding the K-nearest hits for each ellipse center, we check ellipse attendance for them. Eventually, we prolong the accepted candidates and pass them to the model again. As a result, the $O(NK)$ complexity for search continuation of track candidates, where $K \ll N$, is reached. The number of the nearest neighbors is a parameter and plays a significant role, since a small number of NNs gives lower efficiency, but works faster; and the greater the number of NNs, the bigger the efficiency value and the slower the inference.

3 RDGraphNet neural network

Being a local tracking method, the TrackNETv3 model does not allow one to assess the global picture of an event, to see the dependence between individual tracks or groups of tracks and directly recognize phenomena such as secondary vertices. One may also expect the linear dependence of tracking time consumption on the track multiplicity in the event. To overcome these difficulties, a global tracking method based on a Graph Neural Network (GNN) was developed [23].

All hits of an event located at adjacent detector planes are connected by edges, forming a directed graph. Hits become the nodes of this graph. The nodes within one detector layer are not connected. As an illustration, an event in the BM@N detector, represented as a directed graph is shown in Fig. 4.

The graph can be expressed in the form of four matrices:

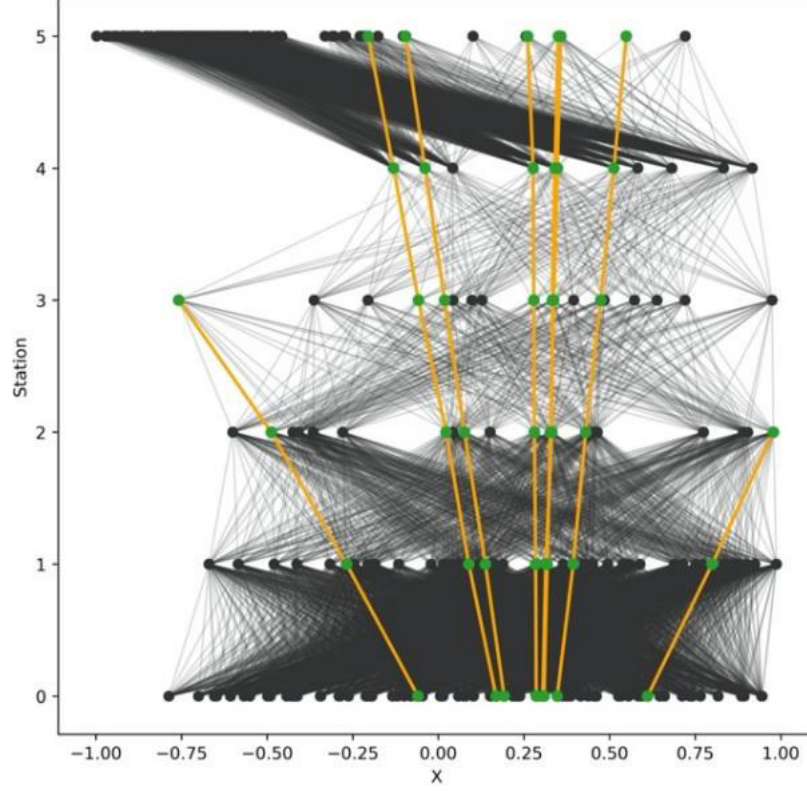


Figure 4: Event in the BM@N detector, represented as a graph. The green nodes are true hits, the black nodes are fakes produced by strip crossings in the GEM-based detector. The orange edges represent real track segments, all the other edges are shown in black.

- X is the matrix of the parameters of nodes of size $N \times M$, where N is the number of nodes, and M is the number of parameters. The hit coordinates are used as node parameters, i.e. $M = 3$.
- R_i is the matrix of incoming edges of size $N \times E$ (E is the number of edges). In this matrix $R_i[i, j] = 1$ if the edge with the index j is included in the node with the index i , otherwise it equals to zero.
- R_o is the matrix of outgoing edges, coming from the corresponding nodes. The matrix has the same properties as R_i .
- Y is the vector with the size E . $Y[j] = 1$ if the edge with the index j belongs to the real track, and zero otherwise.

There are three main components in the GNN: the Input, Node and Edge networks. The Input network is a multilayer perceptron (MLP) with a hyperbolic tangent activation function. The X matrix is fed to the Input network. The goal of the network is to extract from the position of hits some features that will be used later in Edge and Node networks. The output of the Input network is fed to several iterations of "Edge-Node" networks. Any Edge network is a two-layer fully connected

neural network whose task is to calculate the weights of the edges of the graph based on the features of the nodes associated with the corresponding edge. The activation function in the Edge network is a hyperbolic tangent, and the output layer uses a sigmoid activation function to determine whether a graph edge is a true track segment. The Node network is constructed in a similar way, but has a different purpose. This network recalculates the features of the nodes of the graph using the features of neighboring nodes and the weights of all edges coming to and going out from the node, which are obtained by the previous Edge network.

Thus, the initial information in each node of the graph with each iteration is distributed along the edges of the graph, combined with the information of other nodes. The number of such iterations is a global parameter (hyperparameter) of this model. A large number of iterations increases the amount of calculations and affects the performance of the network, but in the same time leads to better network convergence.

If the number of fake hits is high, preprocessing is necessary to reduce the number of fake segments in the final graph. An algorithm of building a reverse directed graph (reverse digraph) is used. The edges of a new graph G_r are the nodes of the original graph G , and the nodes of the reverse graph are the edges of the original one. This approach reduces the number of fake edges by an order of magnitude, while preserving all true edges. To achieve this, the weight for each edge of the graph G_r is calculated by the formula:

$$w_i = \sqrt{(dZ_{i+1} - dZ_i)^2 + (dX_{i+1} - dX_i)^2 + (dY_{i+1} - dY_i)^2}, \quad (3.1)$$

where $dZ_j = Z_j - Z_{j-1}$, $dX_j = X_j - X_{j-1}$, $dY_j = Y_j - Y_{j-1}$ for $i = 1, j \in \{1, 2\}$ and Z_j , X_j and Y_j are the hit coordinates (in the case of a collider experiment, the cylindrical coordinates are used according to 2.2). The training dataset contains only those edges whose weight is $w < 0.073$. This value was chosen during the statistical analysis of training data to keep the maximum number of true edges while minimizing the number of fake edges.

During training, at the input, the network receives a reverse digraph along with labels indicating whether or not the corresponding edge is real or fake. As a result, after training, the RDGraphNet (Reversed Directed Graph Neural Network) neural network predicts the value $x \in [0, 1]$. The true edges of the track candidate are those edges for which x exceeds a certain threshold. Again, the threshold is used for the adjustment of the efficiency and purity of track recognition. In this work, the threshold is fixed and equal to 0.5. The RDGraphNet hyperparameters used for track finding in the planned CGEM detector of the BESIII experiment are summarized in Tab. 2.

Table 2: Training hyperparameters of RDGraphNet.

Parameter	Value
Number of Node-Edge iterations	2
Dimension of input features	5 (coordinates $r_j, r_{j-1}, \varphi_j, \varphi_{j-1}$ & station serial number)
Number of neurons on the hidden MLP layer	96

4 Implementation of neural networks and Ariadne library

The design and performance study of “deep tracking” algorithms described in this work was greatly simplified by using the Ariadne toolkit [28] developed by the authors. The Ariadne toolkit is an open-source Python3 library that aims at solving complex high-energy physics tracking tasks with the help of deep learning methods. Ariadne provides the researcher with a handy framework for the rapid prototyping of a new neural network model for event reconstruction tasks and a step-by-step fully reproducible pipeline including data preparation, training and evaluation phases. Ariadne can use modern deep learning libraries (such as a PyTorch [29], Pytorch Lightning [30]) and allows utilizing multi-core CPU and distributed multi-GPU facilities during preprocessing, training, and performance evaluation. The general structure of the toolkit is shown in Fig. 5.

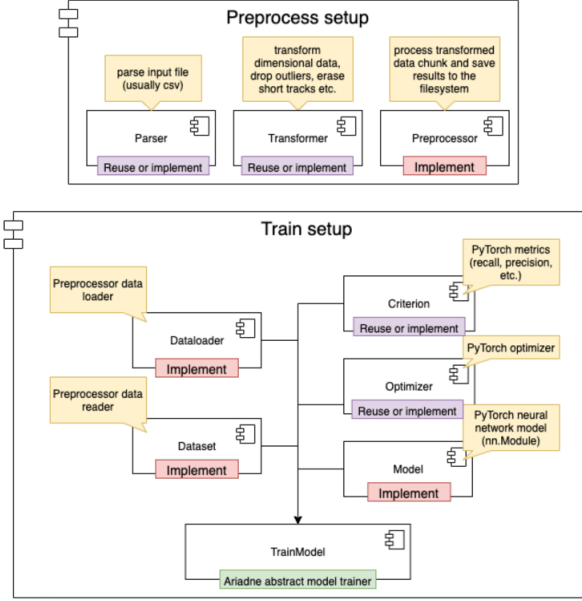


Figure 5: General Ariadne setup process.

The toolkit consists of several modules that allow one to extend it with the details of any experiment setup, to define a neural network model, and describe the user’s data structure, so that one can train and then study the performance of the model and compare it with other models being part of Ariadne. The neural networks described in this work are already implemented in the Ariadne toolkit.

5 Performance study

5.1 Tracking detector of the BM@N experiment

BM@N is a fixed target experiment at the Nuclotron at JINR, aimed at studying the properties of baryon matter formed by the collision of heavy ions at beam energies from 2 to 6 GeV [26]. For this study, the RUN 6 and RUN 7 configurations of the BM@N setup were used. RUN 6 configuration

of the setup contains a central tracker comprising 6 detector planes (stations) of GEM-based strip detectors. Each station has 2 stereo layers with straight and inclined (5-15 degrees) strips. Carbon beam interaction was simulated in the BM@N detector using the BmnRoot framework [27] and the LAQGSM event generator. In total, 550 thousand carbon-carbon (C + C) interactions at a beam energy of 4 GeV were generated. 150 thousand events were considered as a test sample, and the rest of the events were used for training.

Two metrics are used to characterize the performance of the algorithms:

- Hit efficiency: share of true hits found by a network out of all true hits in a single event.
- Track efficiency: share of full tracks without gaps found by a network out of all tracks in a single event.

The results are shown in Tab. 3.

Table 3: Model evaluation results.

	RDGraphNet	TrackNETv2
Track efficiency (%)	87	95.93
Hit efficiency (%)	94	99.18

RUN 7 has a configuration of the detector with 6 GEM stations and 3 silicon stations before the GEM ones, 9 detector planes in total [14]. We generated about 750K events for training and validating the model. We used events with a beam energy equal to 3.2 GeV. Interactions with an argon beam and a plumbum target (ArPb) were considered. The magnet amperage was set to 1250 A. The target was generated with the following parameters: X (mean: 0.7 cm, std: 0.33 cm), Y (mean: -3.7 cm, std: 0.33 cm), Z (center: -1.1 cm, thickness: 0.25 cm). The multiplicity of events varied up to 100 tracks per event, and 37 tracks per event on the average. The number of hits can be more than 500 per station, and about 68% of all hits were fakes.

At the moment, we have trained on BM@N RUN 7 data only the first part of the TrackNETv3 model without a classifier. We normalized the hit coordinates in the dataset depending on the boundaries of the detector area and balanced the size of groups with tracks of different length. In additional, we changed the value of the alpha parameter of the loss function which weights the cost of ellipse fitting to the loss function in opposition to the ellipse area. The optimal value for the “normalized” dataset should be much smaller, otherwise the predicted ellipses will be too large. We set alpha at 0.01.

Two metrics were used to measure the quality of the model:

- Recall: $N_{\text{true}}^{\text{rec}}/N_{\text{MC}}$, where $N_{\text{true}}^{\text{rec}}$ is the number of correctly reconstructed true tracks and N_{MC} – total number of all modelled real tracks (Monte-Carlo).
- Precision: $N_{\text{true}}^{\text{rec}}/N^{\text{rec}}$, where N^{rec} is the total number of reconstructed tracks (including fake tracks).

From the point of view of searching for tracks, the concept of recall coincides with the concept of track recognition efficiency, and precision coincides with the purity of track recognition. The probability that the track found is fake is given by the expression $1 - p$, where p is the precision. The track in our experiment is considered to be correctly reconstructed if 70% of hits or more are found as in the corresponding Monte-Carlo track.

The best results were achieved using 5 nearest neighbors as candidates for entrance in the predicted ellipses. The results are shown in Tab. 4. Time measurements were performed using the Intel (R) Xeon (R) Gold 6148 CPU @ 2.40 GHz for a version of a single-threaded program implemented in Python. Such a large time spread is explained by the fact that in some events there are several hundred thousand candidate tracks that the model should process. The processing can be made much faster by translating the program to a multi-threaded C++ realization.

Table 4: TrackNETv2 model evaluation results on BM@N RUN 7 data.

Track Efficiency (recall) (%)	98.30
Track Purity (precision) (%)	2.09
Mean time to process one event (s)	0.1004 ± 0.1299

5.2 Inner tracker of the BESIII experiment

BESIII [15] is an experiment running at the BEPCII e^+e^- collider at the Institute of High-Energy Physics in Beijing. The physics program of the BESIII experiment [16] covers a wide range of problems, including the study of the τ -lepton, charmed particles and charmonium states. In the BESIII detector, tracks are detected in a drift chamber that consists of two parts: outer and inner one. Currently, the replacement of the inner part, based on Cylindrical GEM detectors, is being developed. The CGEM inner tracker consists of three layers of GEM detectors. The readout anode of each CGEM layer is segmented with 650 μm pitch XV patterned strips. X -strips are parallel to the CGEM axis and provide the ϕ coordinate. V -strips, which have a stereo angle of 30 or 45 degrees to X -strips, define the Z coordinate.

The presented methods were applied to reconstruct tracks in the CGEM-IT detector of the BESIII experiment at a collision energy of 3.686 GeV. We utilized data from the Monte Carlo simulation of electron-positron annihilation events with the formation and decay of the $\psi(3686)$ resonance. For each event, the Monte Carlo simulation produces hits that are either associated with true charged particle tracks or marked as fakes. The procedure for modeling hits is described in detail in work [18]. We used events in which the modeled track always contains three hits, and the tracks do not overlap with each other. The training and validation dataset consisted of 250,000 simulated events.

In the collected dataset, the relative ratio of fake and true hits is $\sim 1:3$ (there are more than 3 fakes per real hit), which adds additional complexity to finding true tracks.

Table 5 contains dataset characteristics for RDGraphNet and TrackNETv3. It should be noted that when training neural network models, only part of the data set described above was used, and the other part formed the validation set.

The parameters used in training neural networks are presented in Tab. 6.

Table 5: Characteristics of datasets used for training and validation.

Characteristics	RDGraphNet	TrackNETv3
Training		
Total no. events	215453	134997
Total no. tracks	1095237	686246
No. hits (including real and fake ones)	11391914	7137867
Fraction of fake hits	77%	77%
Fraction of real hits	23%	23%
Validation		
Total no. events	4326	4326
Total no. tracks	19,653	19,653
No. hits (including real and fake ones)	225321	225321
Fraction of fake hits	77%	77%
Fraction of real hits	23%	23%

Table 6: Hyperparameters used for training.

	RDGraphNet	TrackNETv3
optimizer	Adam [19]	
loss function	<code>torch.nn.functional.binary_cross_entropy</code>	TrackNETv3 loss
learning rate	0.0007	0.001
fakes reweighting real hits reweighting	$W_{false} = w_{false} \cdot 0.555$ $W_{true} = w_{true} \cdot 3$	$W_{false} = w_{false} \cdot 0.625$ $W_{true} = w_{true} \cdot 2.5$

Table 7 shows the results of evaluating the trained models. A track in our experiment always consists of three hits and is considered to be correctly reconstructed if all hits are found as in the corresponding Monte-Carlo track. Figures 6-7 show the dependency of the metrics on the transverse momentum, azimuthal angle and cosine of the polar angle of departure in comparison with the Kalman filter.

Table 7: Model evaluation results.

	RDGraphNet	TrackNETv3
Track Efficiency (recall)	0.9548	0.9475
Track Purity (precision)	0.7404	0.7594
Events fully reconstructed	0.8271	0.8081

The processing speed for the two models, RDGraphNet and TrackNETv3, was measured on the HybriLIT cluster (Intel(R) Xeon(R) Gold 6148 CPU @ 2.40GHz) (see Fig. 8).

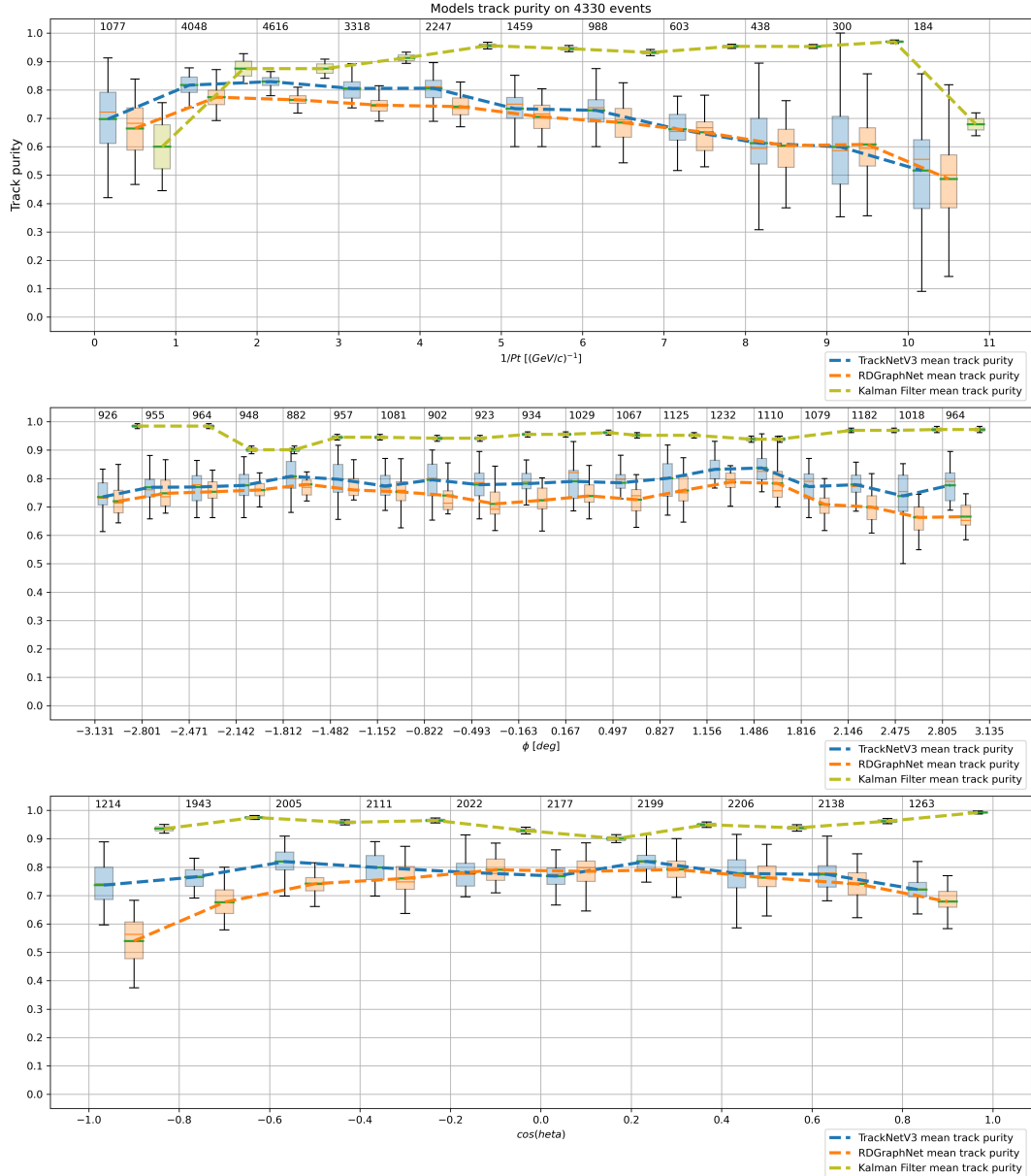


Figure 6: Comparison of TrackNETv3, RDGraphNet and the Kalman filter. Dependence of purity from the transverse momentum, azimuthal angle and cosine of the polar angle of departure (from top to bottom).

6 Conclusion

1. The RDGraphNet neural network model developed on the basis of a reverse digraph for the BM@N experiment with a fixed target, was successfully adapted for the CGEM cylindrical detector of the BESIII collider experiment. Training on Monte-Carlo simulated data and subsequent testing showed encouraging results, namely, $>95\%$ recall and precision $>74\%$

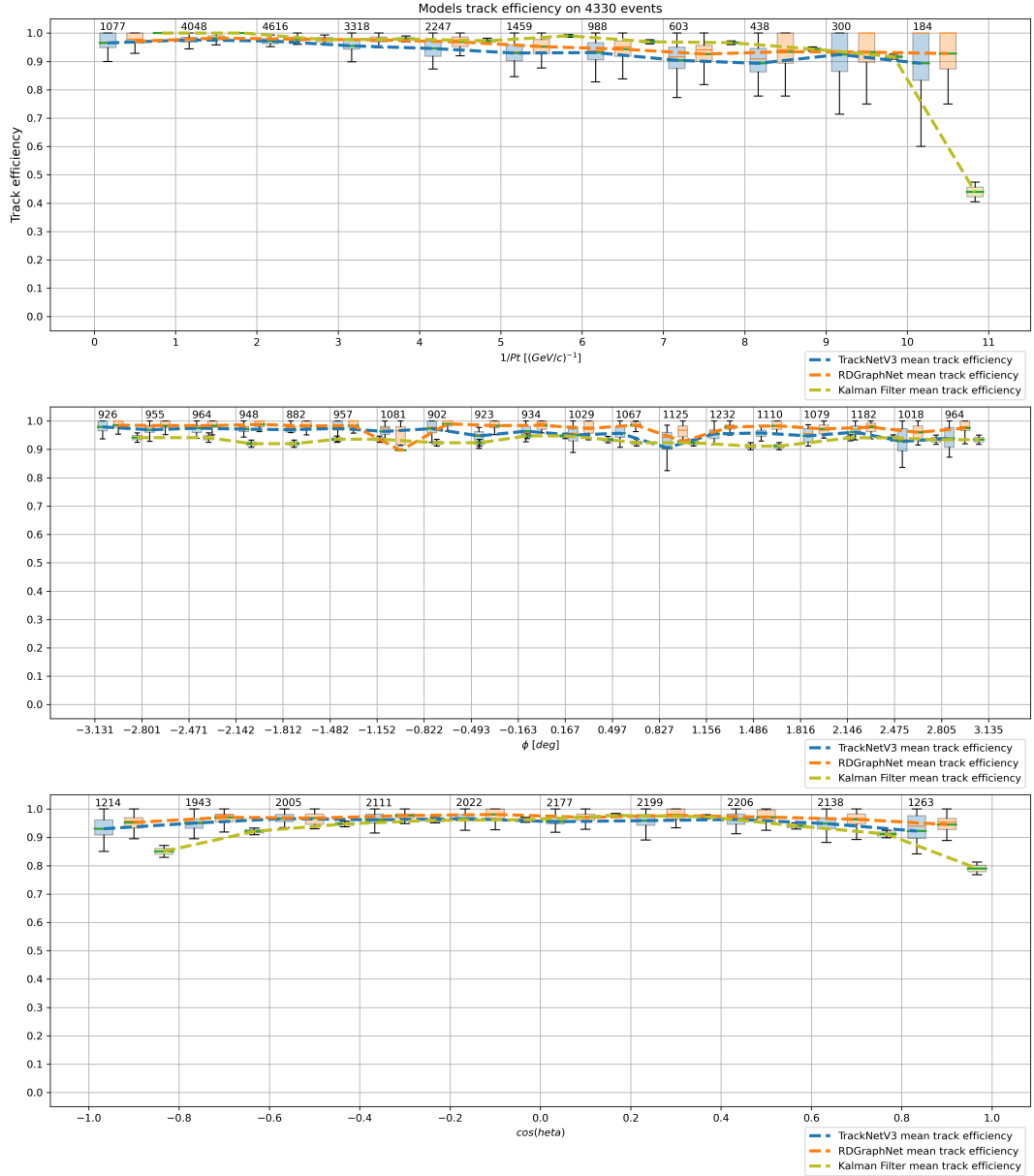


Figure 7: Comparison of TrackNETv3, RDGraphNet and the Kalman filter. Dependence of track efficiency from the transverse momentum, azimuthal angle and cosine of the polar angle of departure (from top to bottom).

precision for both NN approaches.

2. The TrackNETv2 neural network "local" model, developed for the BM@N experiment, was successfully adapted for the CGEM cylindrical detector (BESIII). The resulting program is debugged, trained on simulated data and tested. However, the presence of only three detector stations in the CGEM detector and a large number of fake hits led to the fact that, with the

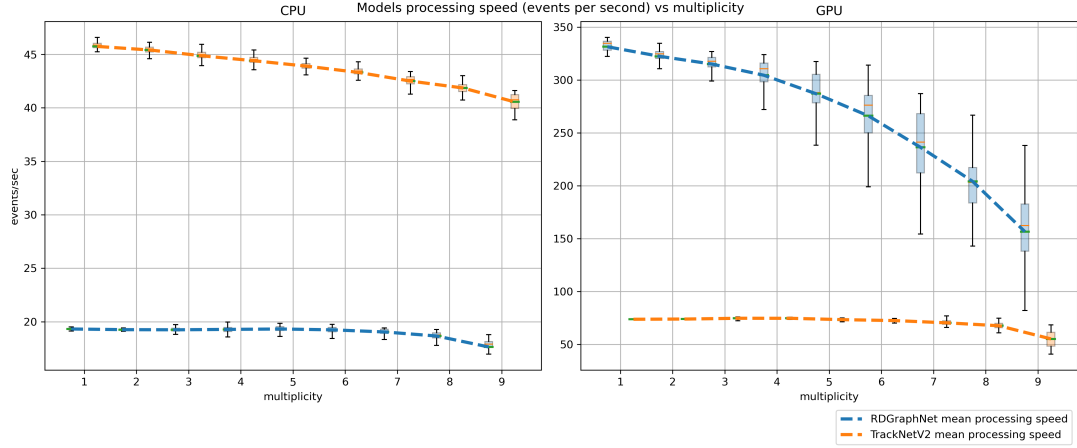


Figure 8: Event processing speed comparison for BESIII between RDGraphNet and TrackNETv3, Python, Single-Threaded

Table 8: Processing speed (number of events processed per second) for each of the models. Test conditions are described in the text of the article.

	RDGraphNet	TrackNETv3
Preprocessing (CPU, Python, single-threaded)	19.28	43.91
Preprocessing (CPU, C++, multithreaded)	570	—
Inference (GPU)	283.70	74.17

achieved high recall of 99% for tracks, the precision was less than 5%. The model recovered many fake tracks. This required the development of additional layers of the neural network that implement a special classifier for filtering out fake tracks, the use of which made it possible to increase the precision up to 75%. The updated version of TrackNET was called TrackNETv3.

3. We revised our TrackNET training approach and optimized the inference procedure using the Faiss library for efficient similarity search to reduce its algorithmic complexity.
4. We trained the regression part of the new TrackNETv3 model on BM@N RUN7 Monte-Carlo data and achieved 98.30% efficiency and 2.09% purity. At the moment, we have not developed a track-candidate classifier that will work as a filter for fake tracks and increase the purity, however, we will develop it in the future. Besides, our preliminary result showed that the TrackNETv3 model was able to process data from experiments with a multiplicity of up to 100 tracks per event.
5. The conversion of the RDGraphNet program written in the Python language into C++ was successfully completed. This gave the acceleration of the tracking process for the internal BES-III detector by 30 times with the same efficiency. The parallel implementation of the

TrackNETv3 model in C++ is under development. It is supposed to optimize programs in terms of memory consumption and speed when using graphics processors.

6. The models proposed in this study can be used as a supplement to the Kalman filter. The achieved purity of the neural models is poor, but the processing speed of even a non optimized Python implementation is rather high and looks promising. Therefore, such programs are expected to operate as intelligent online filters to save disk space during experimental runs. The prospective tracking pipeline will include both novel deep learning models and classical tracking methods. Deep learning models can be responsible for finding good track candidates with higher efficiency, while the Kalman filter will purge redundant tracks with higher purity. These algorithms are general and can be applied to any experiments using strip and pixel tracking detectors, including future experiments at the CEPC collider [32], the SPD experiment at the NICA collider [33], and others that are running or planned.

7 Acknowledgement

The study was carried out with the financial support of the Russian Science Foundation No. 22-12-00109, <https://rscf.ru/project/22-12-00109>.

Supported by the National Natural Science Foundation of China under Contract No. 11911530090.

References

- [1] R. Fruhwirth, *Nucl. Instrum. Meth. A* **262** (1987) 444-450
- [2] B. H. Denby, *Comput. Phys. Commun.* **49** (1988) 429-448
- [3] M. Gyulassy and M. Harlander, *Comput. Phys. Commun.* **66** (1991) 31-46
- [4] D. Baranov, et al., *JINST* **12** (2017) C06041
- [5] G. Mezzadri, *J. Phys. Conf. Ser.* **742** (2016) 012036
- [6] D. Baranov, S. Merts, G. Ososkov and O. Rogachevsky, *EPJ Web Conf.*, **108** (2016) 02012
- [7] D. Baranov, S. Mitsyn, G. Ososkov, P. Goncharov, A. Tsytrinov, *Selected Papers of the 26th International Symposium on Nuclear Electronics and Computing (NEC 2017), Budva, Montenegro, September 25–29, CEUR Proceedings* **2023** (2017) 37–45.
- [8] D. Baranov, G. Ososkov, P. Goncharov, A. Tsytrinov, *EPJ Web of Conferences*, **201** (2019) 05001
- [9] P. Goncharov, G. Ososkov and D. Baranov, *AIP Conf. Proc.* **2163** (2019) 040003
- [10] Dugas C., et al., *Advances in neural information processing systems* (2001) 472–478.
- [11] Xu Bing, et al., *Empirical evaluation of rectified activations in convolutional network* (2015) arXiv:1505.00853
- [12] Goodfellow I., et al., *Deep Learning. MIT Press* (2016) 180–184
- [13] Johnson J., Douze M., Jégou H. *IEEE Transactions on Big Data* (2019)
- [14] Kapishin M. et al., *Nuclear Physics A* (2019) **982** 967-970.
- [15] M. Ablikim *et al.* [BESIII], [arXiv:0911.4960 [physics.ins-det]].
- [16] D. M. Asner, *et al.* *Int. J. Mod. Phys. A* **24** (2009), S1-794 [arXiv:0809.1869 [hep-ex]].

- [17] L. Lavezzi, et al., *JINST* **12** (2017) C07038.
- [18] I. Denisenko and G. Ososkov, *AIP Conf. Proc.* **2163** (2019) 030002
- [19] Kingma Diederik P., Ba Jimmy Lei, arXiv:1412.6980 [cs.LG] — 2014.
- [20] Han Jun, Morag C., From Natural to Artificial Neural Computation. *Lecture Notes in Computer Science.* **930** (1995) 195–201.
- [21] Murphy K., *Machine Learning: A Probabilistic Perspective* (2012)
- [22] T. Lin, Priya G., R. Girshick, K. He and P. Dollar, *Proceedings of the IEEE International Conference on Computer Vision (ICCV)* (2017) 2980-2988.
- [23] E. Shchavalev, P. Goncharov, G. Ososkov, D. Baranov, *Proceedings of the 27th Symposium on Nuclear Electronics and Computing (NEC 2019), Budva, Montenegro, September 30 – October 4, 2019 CEUR Proceedings*, **2507** (2019) 280–284
- [24] P. Goncharov, E. Shchavalev, G. Ososkov, D. Baranov, *EPJ Web of Conferences* **226**, 03009 (2020)
- [25] O. Ronneberger, P. Fischer, T. Brox, *U-net: Convolutional networks for biomedical image segmentation, International Conference on Medical image computing and computer-assisted intervention.* Springer, Cham (2015) 234-241.
- [26] M. Kapishin, et al., *Nuclear Physics A.* **982** (2019) 967-970.
- [27] P. Batyuk, K. Gertsenberger, S. Merts, O. Rogachevsky, *EPJ Web of Conferences*, **214** (2019) 05027.
- [28] Ariadne, <https://github.com/t3hseus/ariadne>
- [29] A. Paszke, et al., *Advances in neural information processing systems* **32** (2019) 8026-8037
- [30] Pytorch-Lightning, <https://pytorchlightning.ai/>
- [31] G. Adam, et al., *Selected Papers of the 8th International Conference “Distributed Computing and Grid-technologies in Science and Education” (GRID 2018), Dubna, Russia.* **2267** (2018) 638-644.
- [32] M. Ahmad, *et al.* IHEP-CEPC-DR-2015-01.
- [33] V. M. Abazov *et al.*, [arXiv:2102.00442 [hep-ex]].